OPTIMIZATION DESIGN AND TEST OF BAFFLE STRUCTURE PARAMETERS OF THE HQ-800 STRAW MILL

/

HQ-800 型秸秆粉碎机隔板结构参数优化设计及试验

Kai YONG [1], Qing TANG [2,3*], Zhewen SONG [3], Lan JIANG [2]

[1]School of Smart Manufacturing, Wuhu Institute of Technology, Wuhu 241006, China;
[2]Nanjing Institute of Agricultural Meshanization, Ministry of Agriculture and Rural Affairs, Nanjing 210014, China;
[3]Sinomach Changlin Co.Ltd., Changzhou 213000, China.
Tel: +86.15366092914; E-mail: tangqing01@caas.cn
DOI: https://doi.org/10.35633/inmateh-76-32

Keywords: *straw mill, baffle, curved optimization, field test*

ABSTRACT

Crop straw is a key feed raw material processed by straw mills, but traditional mills have been hindered bulky structures, high power consumption, and low productivity. Previous research has primarily focused on optimizing the hammer structure, often overlooking the baffle, despite its considerable weight and lack of specific design applications. This study addresses that gap by optimizing the baffle design of the HQ-800 straw mill, simplifying it using a double-baffle framework. The force analysis considered gravity, hammer centrifugal force, shaft centrifugal force, main shaft torque, and material impact. Deformation and stress nephograms revealed that the area between the hammer shaft holes required structural improvement. Two optimization schemes - flat and curved - were compared. The curved design reduced maximum deformation to 29.007 μm, compared to 52.009 μm for the flat design, making it the preferred approach. Key parameters, including cutting circle diameter, center distance, and baffle thickness, were optimized using a three-factor, three-level orthogonal test, resulting in preliminary values of 200 mm, 250 mm, and 12.5 mm, respectively. Subsequent Box–Behnken testing refined these parameters to optimal values: 209 mm, 256 mm, and 12 mm. Under these conditions, the straw mill achieved a productivity of 1673 kg/h and a power consumption of 10.42 kWh/t. Compared to the unoptimized design, the optimized mill reduced volume by 44.46%, increased productivity by 5.89%, and lowered power consumption by 14.10%, fully meeting the design objectives.

摘要

农作物秸秆经粉碎机加工是饲料重要来源，传统粉碎机隔板结构不合理致能耗高、效率低。本文以 HQ-800 型粉碎机隔板为对象，简化模型后进行受力与有限元分析，确定锤轴孔间区域为优化位置，对比方案选弧面优化。通过三因素三水平正交试验得初步参数：切割圆直径 200 mm、圆心距 250 mm、隔板厚度 12.5 mm。Box-Benhnken 试验验证最佳参数为 209 mm、256 mm、12 mm 时，生产率 1673 kg/h，吨料电耗 10.42 kW·h/t，体积减 44.46%，效率提 5.89%，能耗降 14.10%，试验结果满足设计要求，为粉碎机结构优化提供理论支撑。

INTRODUCTION

Feed is the material basis for the development of animal husbandry, providing essential nutrition for herbivorous livestock such as cattle and sheep, and ensuring the high-quality, high-yield and efficient development of animal husbandry. However, the supply of feed raw materials is insufficient, and there has been a long-term reliance on imports *(Zhang et al., 2021; Zartha et al., 2021)*. Crop straw, as one of the feed raw materials, can alleviate the shortage of feed supply if utilized efficiently. Crop straw can be processed into feed through the straw mill, but traditional straw mills have several issues, including a bulky structure, high power consumption and low productivity *(Cao et al., 2021; Cotabarren et al., 2020; Thomas et al., 2018)*. The baffle is the key component in the crushing mechanism of the straw mill, responsible for guiding the straw through the straw mill and ensuring it is effectively crushed and processed. The weight of the baffle typically accounts for more than 50% of the total weight of the crushing mechanism. Therefore, it is necessary to optimize the baffle structure to reduce weight, reduce power consumption and improve productivity.

In recent years, both domestic and international scholars have conducted extensive research on the structural optimization and performance enhancement of crushing-related machinery. *Li et al., (2024),* optimized the process parameters of feed crushing using a back-propagation neural network combined with particle swarm optimization, identifying optimal parameters that significantly improved pulverizer performance.

Ismail et al., (2022), analyzed the synergistic effects of classifier blade lengths and opening angles in coal pulverizers using CFD technology, revealing the classification mechanism by examining the coupling between flow field characteristics and particle movement trajectories. *Kshirsagar et al., (2014),* used finite element analysis software to analyze the stress and deformation of the main components of an automation can/plastic bottle crusher machine, ensuring the stability of the machine. These studies mainly used simulation and machine tests to optimize the structure, and their approaches are worth learning from. However, due to different objects of study, the relevant results cannot be directly applied to straw mill. *Wang et al., (2023),* designed a new type of biomimetic hammer with beaver incisors as biomimetic prototype, and used response surface method to optimize the structural parameters of biomimetic hammer, which showed improved performance compared to conventional hammers. *Zhang et al., (2024),* designed a field returning machine with a biomimetic serrated grinding knife with good straw crushing performance, and when used in combination with traditional crushing knife, it significantly increased the crushing efficiency of the entire machine. *Yancey et al., (2013),* optimized the shape parameters of the mill's hammer, enhancing the crushing performance of the machine. The straw mill is mainly hammer-type, the current optimization focus is mostly on hammers. However, the baffle in the crushing mechanism has a larger weight proportion and is in greater need of optimization. *Ruan et al., (2014),* analyzed the baffle force under both no-material and material conditions of the hammer mill, and verified its strength using simulation software, with results meeting the requirements. *Zhang et al., (2019),* performed topological optimization on the baffle structure with a 50% material removal rate, and used finite element analysis software to conduct static and modal analysis on the optimized structure, obtaining a lightweight baffle that meets strength and stiffness requirements. Overall, research on baffle structural parameter optimization is currently limited, and the few existing studies mainly focus on simulation and verification of specified dimensions, without combining gradual optimization and machine tests in actual working scenarios, lacking a systematic optimization scheme.

In this study, the HQ-800 straw mill was selected as the research subject, with a specific focus on baffle design. Aiming to achieve weight reduction, energy efficiency, and productivity enhancement, the model was simplified, and a comprehensive force analysis was conducted. The structural parameters of the baffle were optimized using finite element simulation, and the proposed improvements were rigorously validated through experimental testing. This research not only provides a strong theoretical foundation but also offers practical guidance for the optimized design of straw mills, contributing to the advancement of agricultural machinery engineering.

MATERIALS AND METHODS

Machine structure

The HQ-800 straw mill is composed of a motor, an air conveying system, a crushing system, and other components (see Figure 1a). The air conveying system includes a lower conveying pipeline, an upper conveying pipeline, an air pump, and a pump chamber. The crushing system, which is central to the machine's operation, consists of a crushing chamber, an advanced crushing mechanism, and a screen. The crushing mechanism comprises a main shaft, 9 baffles, 32 hammer shafts, and 64 hammers (see Figure 1b). The baffles are fixed to the main shaft at specific intervals, providing essential structural support. Each baffle is securely connected to four hammer shafts, and each hammer shaft supports two hammers, which are hinged to allow swinging at a certain angle. This configuration enables efficient impact and pulverization of straw into finer particles.

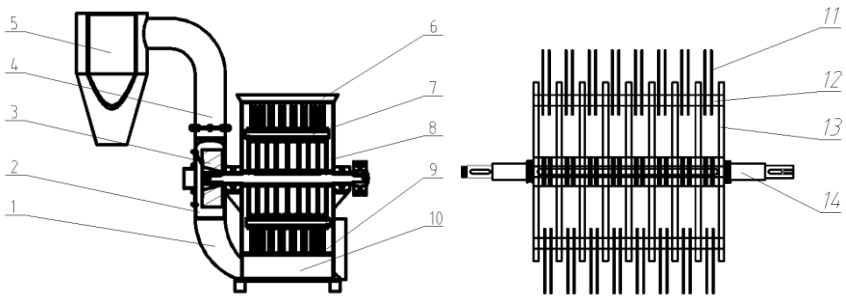

(a) *(b)*

Fig. 1 - Schematic of straw mill

1. lower conveying pipeline; 2. pump chamber; 3. air pump; 4. upper conveying pipeline; 5. discharge port; 6. feed port; 7. crushing mechanism; 8. crushing chamber; 9. screen; 10. material bin; 11. hammer; 12. hammer shaft; 13. baffle; 14. main shaft (a)Straw mill; (b)Crushing mechanism

Working principle

The crushing system is equipped with a feed port, through which crop straws are introduced into the crushing chamber. When the motor is activated, it drives the main shaft via belt transmission. The main shaft then rotates the baffle, which in turn sets the hammers on the hammer shaft into motion. These rotating hammers work in conjunction with the screen to crush the crop straws into feed particles, which subsequently fall into the material bin. Simultaneously, the motor also drives the air pump through the main shaft of the crushing mechanism. The air pump generates air pressure that transports the feed particles from the material bin through both the lower and upper conveying pipelines, ultimately delivering them to the discharge port for packaging. The main technical parameters of the HQ-800 straw mill are listed in Table 1.

Table 1

Main technical parameters

Parameter	Unit	Value
Power	kW	55
Voltage	V	380
Machine size (length×width×heigh)	mm×mm×mm	1800×1500×2000
Maximum speed of main shaft	rpm	2800
Diameter of main shaft	mm	80
Number of hammers	/	64
Feed particle size	mm	2

Design of baffle model

Although the crushing mechanism consists of numerous components, many along the main shaft are highly repetitive. Therefore, two adjacent baffles were selected as the focus of the research and analysis. This section includes four hammer shafts and eight hammers. The simplified baffle model is illustrated in Figure 2.

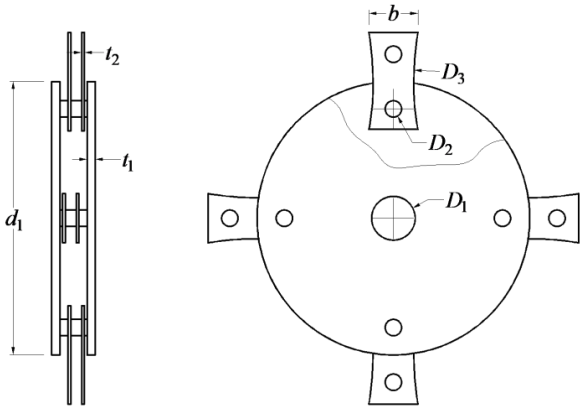

Fig. 2 - Schematic of baffle model

The baffle parameters are as follows: baffle diameter d_1=500 mm, baffle thickness t_1=15 mm, diameter of the main shaft hole D_1=80 mm, and diameter of the hammer shaft hole D_2=30 mm. The hammer features a cambered structure with the following specifications: cambered surface diameter D_3=550 mm, hammer width b=90 mm, and hammer thickness t_2=5 mm.

Force analysis of baffle model

The force analysis of baffle model can be categorized into two types: operation without material and operation with material. In the absence of material, the forces acting on the baffle model primarily consist of the gravity of the baffle model, the friction between the hammer and the hammer shaft, the centrifugal force of the hammer on the hammer shaft, and the torque transmitted by the main shaft *(Liu et al., 2011; Li et al., 2012; Ruan et al., 2014)*. However, when material is present, the impact force of the material on the hammer is added, and the torque transmitted by the main shaft will also change due to the altered load. This results in a more complex force situation for the baffle model, which more accurately reflects the actual operating conditions of the machine. Therefore, the force analysis of the baffle model in the presence of material will be detailed below.

The force analysis diagram of the baffle model is depicted in Figure 3.

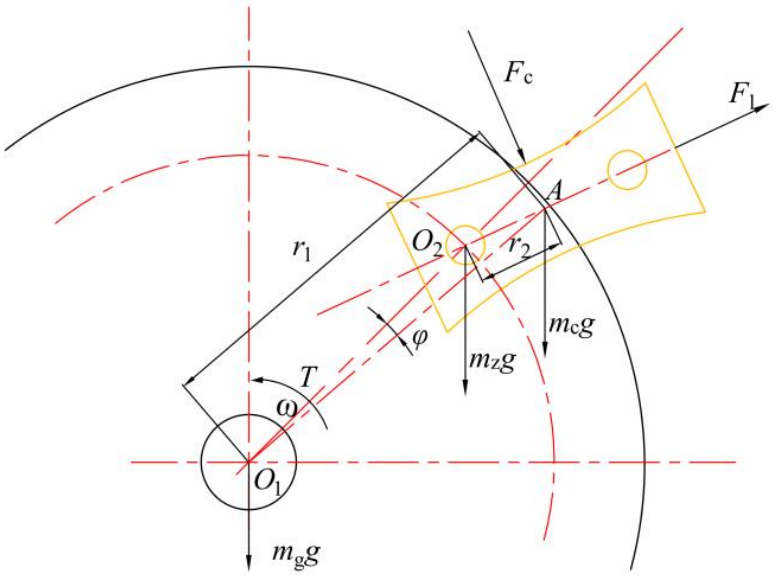

Fig. 3 - Force analysis diagram of baffle model

During the operation of the straw mill, the hammers experience a critical deflection angle $\varphi \approx 3^{\circ}$ relative to the center of the hammer holes *(Ruan et al., 2014)*.

The total weight of the baffle model is the sum of the weights of all its components, and is calculated using Equation (1).

$$G_z = 2m_g g + 4m_z g + 8m_c g \quad (1)$$

where: G_z - total weight of baffle model, [N]; m_g - baffle mass, [kg]; m_z - hammer shaft mass, [kg]; m_c - hammer mass, [kg].

The torque on each baffle is calculated using the following Equations (2) and (3).

$$T_1 = T/9 \quad (2)$$

$$T = 9550 \times \frac{P}{n} \quad (3)$$

where: T_1 - torque on each baffle, [N·m]; T - main shaft torque, [N·m]; n - main shaft rotation speed, [rpm]; P - crushing system power, [kW].

The crushing system power P=20 kW, the main shaft rotation speed n=2000 rpm. It is calculated that the main shaft torque T=95.5 N·m, and the torque on each baffle T_1=10.6 N·m.

Each hammer shaft experiences centrifugal force generated by a hammer, which can be calculated using Equation (4).

$$F_l = m_c \omega^2 r_2 \quad (4)$$

where: F_l - centrifugal force generated by each hammer, [N]; ω - angular velocity of the main shaft, [rad/s]; r_2 - distance from O_2 (the center of the hammer shaft hole) to A (the center of mass of the hammer), [mm].

Under operating conditions with material loaded, the main shaft rotation speed is n=2000 rpm, the hammer mass is m_c =0.16 kg, and the distance from O_2 to A is r_2=50 mm. Based on these values, the angular velocity of the main shaft is calculated as ω=209.33 rad/s, and the centrifugal force generated by each hammer is F_l=350.55 N. Since each hammer shaft is hinged to two hammers, the total centrifugal force acting in one direction of the baffle model is 701.10N.

The hammer experiences the maximum impact force from the material *(Wang et al., 2009)*, and this force is calculated using Equations (5) and (6).

$$F_c = \frac{m_w}{t}(v_c - v_1) \quad (5)$$

$$v_c = \omega r_1 \quad (6)$$

where F_c - maximum impact force exerted by the material on the hammer, [N]; m_w - maximum mass of material carried by a hammer, [kg]; v_c - peripheral velocity of the hammer during impact, [m/s]; v_1 - minimum peripheral velocity of the material during impact, [m/s]; t - minimum collision time [s]; r_1 - distance from O_1 (the center of the main shaft hole) to A (the center of mass of the hammer), [mm].

Under maximum feed conditions, the maximum mass of the material carried by a hammer is m_w=0.1 kg, the distance from O_1 to A is r_1=247 mm, and the peripheral velocity of the hammer is v_c=51.70 m/s. During the feeding process, the material accelerates from an initial state of rest to match the hammer's motion, with its peripheral velocity gradually increasing. Therefore, the minimum peripheral velocity of the material is v_1=0m/s. The collision time typically ranges from 1×10^{-3} to 4×10^{-3} seconds; for this analysis, the minimum collision time is taken as $t=1\times10^{-3}$ s. It is calculated that the maximum impact force is F_c=5170 N.

Model settings of simulation test

Simulation testing is a widely used method in structural optimization design, employing techniques such as static analysis, dynamic analysis, and fluid mechanics to evaluate the physical behavior of the designed structure *(Wu et al., 2023; Wang et al., 2024)*. In this study, the 3D model was imported into ANSYS Workbench. The materials were assigned as follows: Q235 for the baffle and hammer shafts, and 65Mn for the hammers. A Body-Ground Revolute constraint was applied to the virtual main shaft, while a Body-Body Revolute constraint was used between the hammer and hammer shaft. The mesh size was set to 5 mm. The resulting mesh, shown in Figure 4, consists of 488,740 nodes and 99,252 elements, with an average mesh quality of 91.87%.

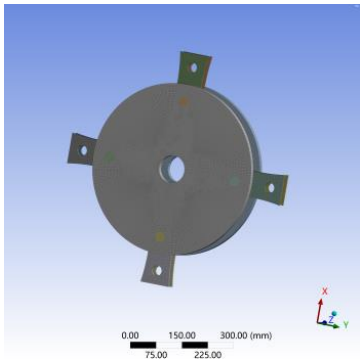

Fig. 4 - Schematic of grid model

Optimization method of baffle structure

As shown in Figure 5, the baffle structure can be optimized using either flat-surface removal or curved-surface removal. Two models are proposed, each removing the same volume of material, while maintaining the original installation configuration of the baffle, hammer shaft, and hammers. In the first model, the baffle corners are removed in a sector shape, resulting in a "cross"-shaped remaining structure (see Figure 5a). In the second model, the baffle corners are removed in an oval shape (see Figure 5b).

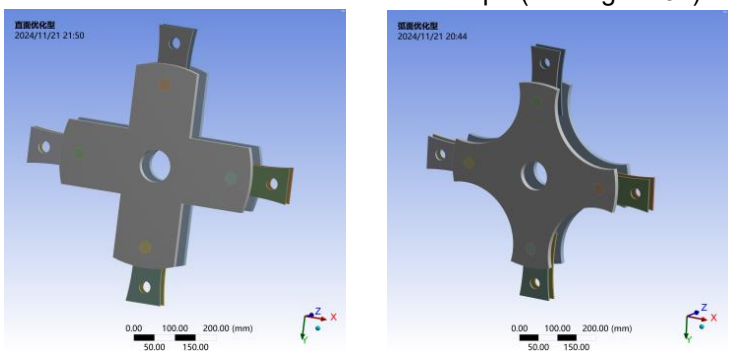

(a) *(b)*

Fig. 5 - Schematics of optimized contrastive baffle model

(a)Flat-optimized baffle model; (b)Curved-optimized baffle model

Simulation parameter optimization of baffle structure

During the operation of the straw mill, the maximum deformation of the components in the crushing mechanism affects the efficiency of the machine. *Xu et al., (2021),* conducted a study on the maximum deformation of key components in the crushing mechanism. Combining this with the team's prior analysis and tests, it was found that when the maximum deformation of the baffle reaches 35 μm, the efficiency of the machine significantly decreases, and malfunctions are more likely to occur. Referring to the unoptimized baffle model, the maximum deformation is 27.803 μm. It is recommended that the simulation analysis reference index should not exceed 5% of this value, and the smaller the maximum deformation, the better.

Combining the topological optimization study of the baffle by *Zhang et al., (2019),* the curved-optimized scheme can cut the four corners of the baffle along a curve, but it is necessary to avoid the hammer shaft hole and maintain a certain distance from the main shaft hole. Considering that the parameters of a variable-curvature curve are numerous and have minimal impact on the optimization results, four equal-diameter circular arcs are used to trim the edges of the baffle. The optimization parameters of the curved-optimized baffle are shown in Figure 6, where the main shaft hole is located at the center of the baffle, and the four hammer shaft holes are located at the edges of the baffle, the center distance *L* between the center of the baffle and the center of the cutting circle, and the cutting circle diameter *D*, together affect the amount of baffle removal. In addition, the baffle thickness *t* also has a significant impact. Therefore, the main optimization parameters of the baffle include the cutting circle diameter, the center distance, the baffle thickness, the diameter of the main shaft hole, and the diameter of the hammer shaft hole.

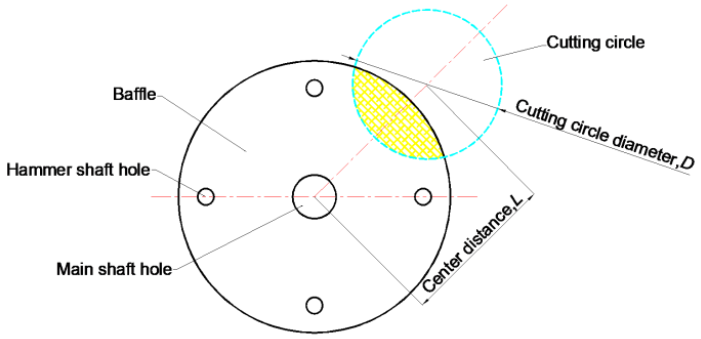

Fig. 6 - Optimization parameters of curved-optimized baffle

In accordance with the assembly requirements of the crushing mechanism, the baffle's main shaft hole and hammer shaft holes are precisely fitted with the main shaft and hammer shafts, respectively. In the early lightweight design of the main shaft and hammer shafts, their dimensions have already been optimized to the minimum. Increasing the diameters of the main shaft hole and hammer shaft holes could reduce the mass of the baffle but would also increase the mass of the main shaft and hammer shafts, thereby negatively impacting the overall performance of the crushing mechanism. Therefore, the optimization analysis of the baffle only considers three factors: the cutting circle diameter, the center distance, and the baffle thickness. The evaluation indexes are selected as the maximum deformation and the volume reduction ratio. The maximum deformation is the greatest deformation of the baffle caused by the force when it is in operation with material, while the volume reduction ratio is calculated as (The volume of the unoptimized baffle - The volume of the optimized baffle for each test group) / The volume of the unoptimized baffle. The volume reduction ratio reflects the optimization rate of the baffle structure for each test group. Considering the structural characteristics of the baffle, the table of test factors is presented in Table 2. The orthogonal test method with three factors and three levels is adopted *(Wang et al., 2017; Li et al., 2024)*, and the simulation results are shown in Figure 9.

Table 2

Table of test factors

Number	Factors		
	Cutting circle diameter A, (mm)	Center distance B,(mm)	Baffle thickness C,(mm)
1	150	200	10
2	200	250	12.5
3	250	300	15

Field test standard

The tests are conducted in accordance with the standards GB/T 6971-2007 "Test Method for Feed Mills" and NY/T 1554-2007 "Technical Specification of Quality Evaluation for Feed Grinder"

These standards clearly specify the evaluation indexes for the performance of straw mill, which include productivity, power consumption, feed particle size, feed temperature rise, motor load, noise, and dust concentration. Based on the results of the previous tests, it was found that the optimized baffle structure primarily affects the first two performance evaluation indexes.

The feed production per unit time of the straw mill is termed the productivity, and is calculated using Equation (7).

$$E = \frac{M}{t_1} \tag{7}$$

where: E - productivity, [kg/h]; M - feed production during test time, [kg]; t_1 - test time, [h].

The energy consumption required for the straw mill to produce each ton of feed is termed the power consumption, and is calculated using Equation (8).

$$W = \frac{W_n}{M/1000} \tag{8}$$

where: W- power consumption, [kWh/t]; W_n - energy consumption during test time, [kW·h].

RESULTS

Simulation results

As shown in Figure 7a, the maximum deformation was mainly concentrated around the main shaft hole and the hammer shaft holes, with the maximum deformation being 27.803 μm. There were some positions between the hammer shaft holes of the baffle where the deformation was relatively low, which could be considered for optimization and removal. Figure 7b showed that the positions of the stress concentration were consistent with the positions of the deformation. Therefore, the positions between the hammer shaft holes of the baffle could be optimized and removed.

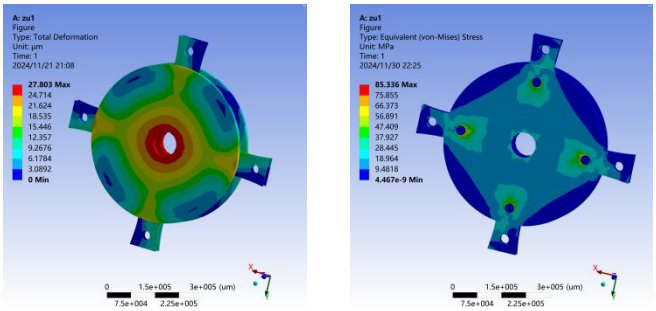

(a) *(b)*

Fig. 7 - Total deformation and stress nephogram of baffle model

(a)Total deformation nephogram; (b)Stress nephogram

As shown in Figure 8a, the flat-optimized scheme reduced the baffle volume, but the contour transition was poor, leading to stress concentrations close to the main shaft center. The maximum deformation was concentrated at the main shaft hole and the hammer shaft holes, with the maximum deformation reaching 52.009 μm. In Figure 8b, the curved-optimized scheme offered a more coordinated contour, also significantly reduced the baffle volume, and was less likely to produce noticeable stress concentrations. The maximum deformation was 29.007 μm, with a small increase in deformation. Therefore, the curved-optimized scheme could ensure a significant reduction in baffle volume while maintaining a small increase in deformation.

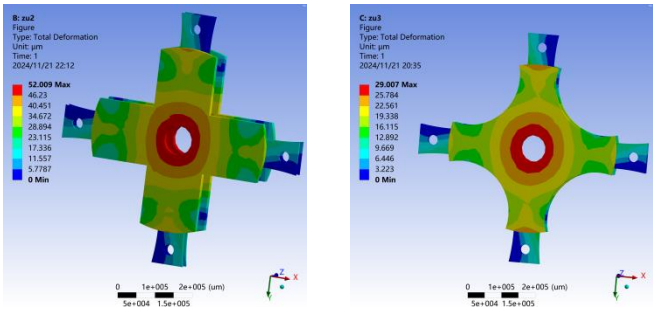

(a) *(b)*

Fig. 8 - Contrastive nephogram of total deformation

(a) Flat-optimized baffle model; (b) Curved-optimized baffle model

As shown in Figure 9, the distribution trend of the maximum deformation across the nine sets of curved-optimized baffles aligned well with the structural optimization logic. The highest deformation was concentrated around the main shaft hole and hammer shaft holes, while smaller deformations appeared near the material removal regions. The simulation results were consistent with the force analysis outcomes. Although the amount of material removed increased, the maximum deformation did not exhibit a strictly linear growth. This indicates that the relationship among the three influencing factors and the maximum deformation is complex and requires further analysis.

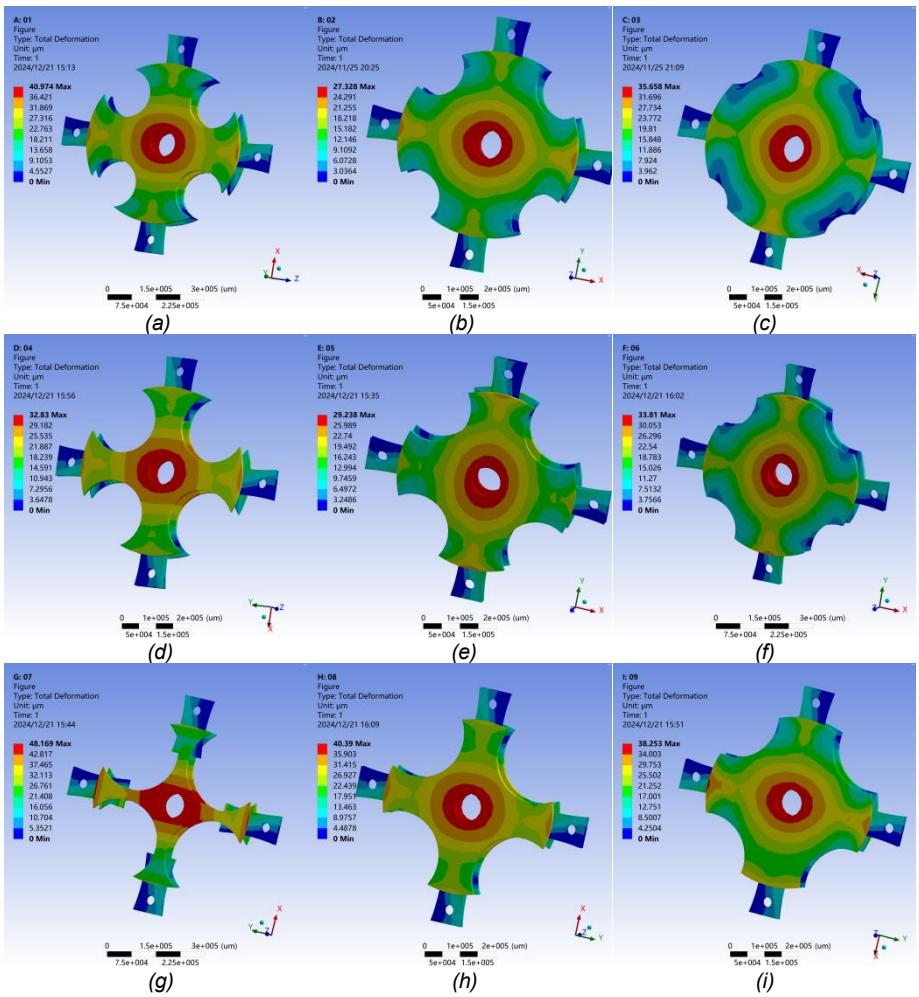

Fig. 9 - Contrastive nephogram of total deformation of curved-optimized type
(a) test 1; (b) test 2; (c) test 3; (d) test 4; (e) test 5; (f) test 6; (g) test 7; (h) test 8; (i) test 9

Analysis of simulation results

The test scheme and results are presented in Table 3. Through range analysis, the factors influencing the maximum deformation of the baffle were identified as the cutting circle diameter, the center distance, and the baffle thickness. The optimal combination of these factors was found to be $A_2B_2C_2$, corresponding to a cutting circle diameter of 200 mm, a center distance of 250 mm, and a baffle thickness of 12.5 mm. Comparison of the volume reduction ratios revealed that the maximum deformation was not directly proportional to the volume reduction, indicating that the volume reduction ratio should be used as a secondary evaluation index. Variance analysis was conducted to test the significance of the impact of each factor on the maximum deformation, as shown in Table 4. The results confirmed that the cutting circle diameter, the center distance, and the baffle thickness have a significant effect on the maximum deformation, validating the rationality of the orthogonal test.

Table 3

Test scheme and results of simulation analysis

Test number	Factors			Baffle volume (mm^3)	Volume reduction ratio (%)	Maximum deformation (μm)
	Cutting circle diameter A, (mm)	Center distance B, (mm)	Baffle thickness C, (mm)			
1	150	200	15	1899824	32.8	40.974
2	150	250	12.5	1942597	31.3	27.328
3	150	300	10	1815645	35.8	35.658
4	200	200	12.5	1143800	59.5	32.830
5	200	250	10	1310187	53.7	29.238

Test number	Factors			Baffle volume (mm^3)	Volume reduction ratio (%)	Maximum deformation (μm)
	Cutting circle diameter A, (mm)	Center distance B, (mm)	Baffle thickness C, (mm)			
6	200	300	15	2504307	11.4	33.810
7	250	200	10	512190	81.9	48.169
8	250	250	15	1512059	46.5	40.390
9	250	300	12.5	1824638	35.5	38.253
Maximum deformation			K_1	34.65	40.66	38.39
			K_2	31.96	32.32	32.80
			K_3	42.27	35.91	37.69
			R	10.31	8.34	5.59
			Better level	A_2	B_2	C_2
			Effects of various factors		$A > B > C$	

Table 4

Analysis of variance of maximum deformation

Source of variance	Sum of variance	Degree of freedom	F value	P value	Significance
A	171.60	2	1452.13	0.001	***
B	104.98	2	888.38	0.001	***
C	55.58	2	470.29	0.002	**
Pure Error	0.12	2			

*Note: *** indicates an extremely significant effect (P < 0.01); ** indicates a significant effect (P < 0.05). The same applies below.*

Field test scheme and results

The test site was a corn planting test field, and the test machine was the HQ-800 straw mill. The test material was corn straw, with a length of approximately 400 mm and a moisture content controlled between 12% and 18%. The material contained no other impurities. The main shaft speed of the test machine was set at 2000 rpm, and each test lasted 20 minutes. The test was repeated three times, and the average value was taken.

Based on the simulation analysis results, further verification of the effects of cutting circle diameter, center distance, and baffle thickness on the performance of the straw mill was conducted through machine tests. The coding of test factors is presented in Table 5. The performance evaluation indicators for the straw mill are productivity and power consumption.

Table 5

Coding of test factors

Level	Factors		
	Cutting circle diameter A, (mm)	Center distance B,(mm)	Baffle thickness C,(mm)
-1	150	200	10
0	200	250	12.5
1	250	300	15

The completely randomized test design was developed by coding the cutting circle diameter, center distance and baffle thickness as test factors *(Wen et al., 2023; Zhang et al., 2022).* The test scheme and results are presented in Table 6.

Table 6

Test scheme and results

Test number	Factors			Productivity E, (kg·h^{-1})	Power consumption W, (kWh·t^{-1})
	Cutting circle diameter A, (mm)	Center distance B, (mm)	Baffle thickness C, (mm)		
1	-1	-1	0	1546	11.64
2	1	-1	0	1583	11.05
3	-1	1	0	1572	11.25
4	1	1	0	1603	11.12
5	-1	0	-1	1585	11.25
6	1	0	-1	1628	10.98
7	-1	0	1	1558	11.45
8	1	0	1	1594	11.08
9	0	-1	-1	1604	11.11
10	0	1	-1	1623	11.02
11	0	-1	1	1578	11.22
12	0	1	1	1602	10.68
13	0	0	0	1675	10.38
14	0	0	0	1677	10.28
15	0	0	0	1676	10.25
16	0	0	0	1665	10.44
17	0	0	0	1673	10.41

The Box-Behnken Design (BBD) module in Design-Expert software was utilized to analyze the test data. The outcomes of this analysis are detailed in Tables 7 and 8. The regression model expressing the relationship between the productivity, the power consumption, and the encoded values is provided below:

$$E=1673.20+18.38A+11.13B-13.50C-1.5AB-1.75AC+1.25BC-53.85A^2-43.35B^2-28.10C^2 \quad (8)$$

$$W=10.35-0.089A-0.026B-0.060C+0.140AB+0.313AC+0.053BC+0.554A^2+0.384B^2+0.322C^2 \quad (9)$$

The regression models for productivity and power consumption were found to be extremely significant ($P < 0.01$). The P values for the lack of fit were 0.6558 and 0.2163, respectively, both of which were non-significant ($P > 0.1$), indicating a high degree of model fit. As shown in Table 7, the cutting circle diameter, center distance, and baffle thickness had extremely significant effects on productivity, with the cutting circle diameter having the greatest impact, followed by baffle thickness and then center distance. Table 8 indicates that the cutting circle diameter had an extremely significant effect on power consumption, while the center distance had a significant effect and the baffle thickness had a non-significant effect. The order of influence was cutting circle diameter, center distance, and baffle thickness. The determination coefficients (R^2) for the regression models of productivity and power consumption were 0.9957 and 0.9743, respectively, indicating excellent model fit. The adjusted determination coefficients (Adjusted R^2) were 0.9902 and 0.9413, respectively, which are close to the R^2 values, suggesting strong correlations. These results confirm the validity and reliability of the test design and analysis.

Table 7

Analysis of variance of productivity

Source of variance	Sum of variance	Degree of freedom	Mean square deviation	F value	P value	Significance
Model	31145.51	9	3460.61	181.39	< 0.0001	***
A	2701.13	1	2701.13	141.58	< 0.0001	***
B	990.13	1	990.13	51.90	0.0002	***
C	1458.00	1	1458.00	76.42	< 0.0001	***
AB	9.00	1	9.00	0.4717	0.5143	
AC	12.25	1	12.25	0.6421	0.4493	
BC	6.25	1	6.25	0.3276	0.5850	
A^2	12209.78	1	12209.78	639.97	< 0.0001	***
B^2	7912.52	1	7912.52	414.73	< 0.0001	***
C^2	3324.67	1	3324.67	174.26	< 0.0001	***
Residual	133.55	7	19.08			
Lack of Fit	40.75	3	13.58	0.5855	0.6558	
Pure Error	92.80	4	23.20			
Cor Total	31279.06	16				

Table 8

Analysis of variance of power consumption

Source of variance	Sum of variance	Degree of freedom	Mean square deviation	F value	P value	Significance
Model	2.86	9	0.3180	29.52	< 0.0001	***
A	0.2312	1	0.2312	21.46	0.0024	***
B	0.1128	1	0.1128	10.47	0.0143	**
C	0.0006	1	0.0006	0.0569	0.8184	
AB	0.0529	1	0.0529	4.91	0.0622	
AC	0.0025	1	0.0025	0.2321	0.6447	
BC	0.0506	1	0.0506	4.70	0.0668	
A^2	1.26	1	1.26	117.27	< 0.0001	***
B^2	0.5617	1	0.5617	52.15	0.0002	***
C^2	0.3547	1	0.3547	32.93	0.0007	***
Residual	0.0754	7	0.0108			
Lack of Fit	0.0479	3	0.0160	2.33	0.2163	
Pure Error	0.0275	4	0.0069			
Cor Total	2.94	16				

Analysis of field test results

To further analyze the effects of each factor on productivity and power consumption, two-factor response surfaces were generated using Design-Expert software. The response surface for productivity of baffle thickness and cutting circle diameter is shown in Figure 10a. As the cutting circle diameter increases from 150 mm to 250 mm, the baffle volume decreases, and productivity first increases steadily and then gradually decreases. This is because, when the cutting circle diameter is small, increasing its size results in more material being removed from the baffle, reducing the mass of the crushing mechanism. With constant input power, the straw mill can then allocate more energy to the actual crushing of straw, thereby increasing productivity. However, once the cutting circle diameter reaches a certain value, further increases in size lead to a decrease in the baffle's stiffness and other mechanical properties, which reduces the straw mill performance and thus productivity. As the baffle thickness increases from 10 mm to 15 mm, the baffle volume increases, and productivity first increases and then decreases. Response surface for power consumption of center distance and cutting circle diameter is shown in Figure 10b. As the cutting circle diameter increases from 150 mm to 250 mm, the baffle volume decreases, and power consumption first decreases and then increases. Similarly, as the center distance increases from 200 mm to 300 mm, the baffle volume increases, and power consumption first decreases and then increases.

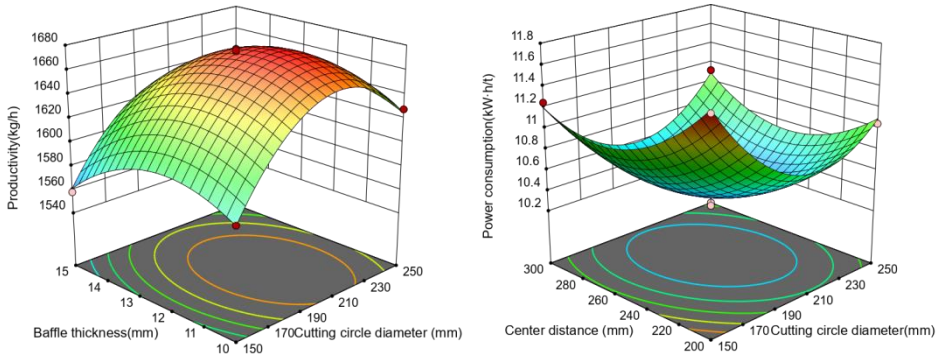

(a) *(b)*

Fig. 10 - Response surface for productivity and power consumption

(a) Response surface for productivity of baffle thickness and cutting circle diameter;
(b) Response surface for power consumption of center distance and cutting circle diameter

Based on the test data and as shown in Figure 10, the optimal productivity of 1677.105 kg/h and power consumption of 10.352 kW·h/t were achieved when the cutting circle diameter was 208.638 mm, the center distance was 256.123 mm, and the baffle thickness was 11.892 mm. These values closely aligned with the simulation results. Considering the manufacturing characteristics for the baffle, the dimensions were rounded to the nearest whole numbers, resulting in a final optimized cutting circle diameter of 209 mm, a center distance of 256 mm, and a baffle thickness of 12 mm. The baffle with the final optimized dimensions was tested on the machine, with each test repeated three times to obtain the average values. The test results were then compared to those of the unoptimized baffle, as shown in Table 9.

Table 9

Contrastive analysis of before and after optimization

Baffle Structure	Baffle volume (mm^3)	Maximum deformation (μm)	Productivity ($kg \cdot h^{-1}$)	Power consumption ($kWh \cdot t^{-1}$)
Unoptimized	2827433	27.803	1580	12.13
Finally optimized	1570436	28.525	1673	10.42
Rate of change(%)	-44.46	+2.60	+5.89	-14.10

As shown in Table 9, the finally optimized baffle volume was significantly reduced, while the maximum deformation slightly increased but remained within the allowable range. Productivity slightly improved, and power consumption was notably reduced. These results indicate that the optimization logic for the baffle structure is rational and the optimization effect is satisfactory.

CONCLUSIONS

Based on the domestic and international status quo analysis of straw mill, the baffle was identified as the target for optimization. A simplified double-baffle model was established. Through force analysis of the baffle model under material conditions, the force parameters of the baffle model were obtained, including the gravity of the baffle model, the impact force of the material on the hammer, the centrifugal force of the hammer, and the torque transmitted by the main shaft.

Finite element analysis software was used to simulate the baffle model. Based on the total deformation and equivalent stress nephogram, it was determined that the positions between the hammer shaft holes on the baffle could be optimized. Comparing the flat-optimized and curved-optimized schemes, it was found that under the same volume removal conditions, the curved-optimized baffle resulted in a smaller increase in maximum deformation and allowed for greater volume optimization.

Further finite element analysis tests were conducted, with the cutting circle diameter, center distance, and baffle thickness as the three factors in an orthogonal test design, and the maximum deformation as the evaluation index. The preliminary optimized dimensions of the baffle were determined to be a cutting circle diameter of 200 mm, a center distance of 250 mm, and a baffle thickness of 12.5 mm.

The machine tests were conducted using the Box-Behnken test design method. Productivity and power consumption were used as evaluation indexes. Considering the manufacturing characteristics of the baffle structure, the optimal combination was found to be a cutting circle diameter of 209 mm, a center distance of 256 mm, and a baffle thickness of 12 mm. The finally optimized baffle achieved a productivity of 1673 kg/h and a power consumption of 10.42 kWh/t. Compared to the unoptimized baffle, the finally optimized baffle volume was reduced by 44.46%, productivity increased by 5.89%, and power consumption decreased by 14.10%, demonstrating a significant improvement in overall performance.

ACKNOWLEDGEMENT

This research was supported by Anhui provincial quality engineering project, 2024jyxm0909; Anhui provincial college and university scientific research project, 2024AH052010; Wuhu institute of technology innovation team project, wzykytd202403; Wuhu institute of technology scientific research project, wzyzrzd202507.

REFERENCES

[1] Cao L.Y., Li S.B., Li C.D., Wang Y., Wang F. (2021). The research and development status of hammer feed mill (锤片式饲料粉碎机的研究发展现状). *Feed Industry*. Vol. 42, no. 3, pp. 31-36, Liaoning/China.

[2] Cotabarren I., Fernandez M.P., Di Battista A., Piña J. (2020). Modeling of maize breakage in hammer mills of different scales through a population balance approach. *Powder Technology*. Vol. 375, pp. 433-444, Switzerland.

[3] Ismail F.B., Al-muhsen N.F.O., Hasini H. (2022). Computational Fluid Dynamics (CFD) investigation on associated effect of classifier blades lengths and opening angles on coal classification efficiency in coal pulverizer. *Case Studies in Chemical and Environmental Engineering*. Vol. 6, pp. 100266, Britain.

[4] Kshirsagar V.N., Choudary D.S.K., Misname A.P. (2014). Experimentation and analysis of an automation can/plastic bottle crusher machine. *International journal for innovation research in science & technology*. Vol. 1, no.2, pp. 1-5, India

[5] Li C.D., Zhou Y., Cao L.Y., Bai Y.Q., Wang Y. (2024). Multi-objective optimization design of feed crushing process parameters (饲料粉碎过程工艺参数多目标优化设计). *Feed Research*. Vol. 47, no.5, pp.127-132, Beijing/China.

[6] Liu B., Zong L., Zhang D.X. (2011). Force and motion states of hammer mill at unloaded running (锤片式粉碎机空载运行中锤片的受力及运动状态). *Transactions of the Chinese Society of Agricultural Engineering*. Vol. 27, no.7, pp. 123-128, Beijing/China.

[7] Li G.Q., Guo X.R. (2012). Design and research on hammer of hammer mill (锤片式粉碎机锤片的设计与研究). *Agricultural Technology & Equipment*. no.5, pp. 38-40, Shanxi/China.

[8] Li C.D., Liu Y., Cao L.Y., Bai Y.Q., Wang F., Zhang S.W. (2024). Experimental research on optimization of working parameters of hammer mill (锤片式粉碎机工作参数优化试验研究). *Journal of Chinese Agricultural Mechanization*. Vol. 45, no.2, pp. 122-129, Jiangsu/China.

[9] Ruan J.L., Zhang L. (2014). Intensity analysis of the hammer framework of hammer mill (锤片式粉碎机锤架板强度分析). *Food & Machinery*. Vol. 30, no.6, pp. 82-84, 237, Hunan/China.

[10] Ruan J.L., Zhang L., Zeng G.L. (2014). The dynamic analysis on the closed rotor of hammer mill (锤片粉碎机封闭式转子结构的动力学分析). *Cereal & Feed Industry*. no.10, pp. 43-45, 54, Hubei/China.

[11] Thomas M., Hendriks W.H., van der Poel A.F.B. (2018). Size distribution analysis of wheat, maize and soybeans and energy efficiency using different methods for coarse grinding. *Animal Feed Science and Technology*. Vol. 240, pp. 11-21, Netherlands

[12] Wang J.D., Xie Y.H., Chen Y., Wu Z.Y. (2023). Biomimetic design of hammer pieces for hammer mill based on beaver incisors (基于河狸门齿的锤片式粉碎机锤片仿生设计). *Chinese Journal of Engineering Design*. Vol. 30, no.4, pp. 476-484, Zhejiang/China.

[13] Wang Y.C., Yu X.G. (2009). Main methods to improve crushing efficiency of sieve hammer mill (提高有筛锤片粉碎机粉碎效率的主要途径). *Feed Industry*. Vol. 30, no.17, pp. 1-4, Liaoning/China.

[14] Wu W.X., Yu X.L., Zhang Z.C., Li Q., Sun Q.Y., Zhao F., Jia Z.C. (2023). Improved design of the classification structure of vertical mechanical impact superfine grinder (立式机械冲击式超微粉碎机分级结构的改进设计). *Transactions of the Chinese Society of Agricultural Engineering*. Vol. 39, no.12, pp. 245-253, Beijing/China.

[15] Wang P.F., Xu S., Yang X., Li S.K. (2024). Optimization design and test of air delivery system for tower sprayer (塔形喷雾机风送系统优化设计与试验). *Transactions of the Chinese Society for Agricultural Machinery*. Vol. 55, no.11, pp. 342-351, 390, Beijing/China.

[16] Wang D.F., Wang M., Li L.Q. (2017). Mechanism analysis and parameter optimization of hammer mill for corn stalk (锤片式粉碎机粉碎玉米秸秆机理分析与参数优化). *Transactions of the Chinese Society for Agricultural Machinery*. Vol. 48, no.11, pp. 165-171, Beijing/China.

[17] Wen X.Y., Hong Y.M., Xiong J.M., Yu Y.G., Tan J.H., Meng X.B. (2023). Design and experiment of fixed automatic natural rubber tapping machine (固定式天然橡胶自动割胶机设计与试验). *Transactions of the Chinese Society for Agricultural Machinery*. Vol. 54, no.z2, pp. 128-135, Beijing/China.

[18] Xu W., Cao C.P., Sun Yu. (2021). Optimization design of hammer structure parameters of hammer mill (锤片式粉碎机锤片结构参数优化设计). *Journal of Agricultural Mechanization Research*. Vol. 43, no.1, pp. 27-33, Heilongjiang/China

[19] Yancey N., Wright C.T., Westover T.L. (2013). Optimizing hammer mill performance through screen selection and hammer design. *Biofuels*. Vol. 4, no.1, pp. 85-94, Britain

[20] Zhang X.R., Cao C., Zhang L.N., Xing J.J., Liu J.X., Dong X.H. (2022). Design and test of profiling progressive natural rubber automatic tapping machine (仿形进阶式天然橡胶自动割胶机设计与试验). *Transactions of the Chinese Society for Agricultural Machinery*. Vol. 53, no.4, pp. 99-108, Beijing/China.

[21] Zhang Y.X., Wang G.G., Tao S., Xu W.P. (2021). Development status, future trend and countermeasures of feed industry in 2020 (2020 年饲料产业发展状况、未来趋势及对策建议). *Chinese Journal of Animal Science*. Vol. 57, no.6, pp. 265-268, Beijing/China.

[22] Zhang X.R., Ni S.L., Liu J.X., Hu X.H., Zhang Z.F., Fu S.H. (2024). Design and flow field analysis of bionic blade of banana straw crushing and throwing machine (香蕉秸秆粉碎抛撒还田机仿生刀片设计与试验). *Transactions of the Chinese Society for Agricultural Machinery*. Vol. 55, no.8, pp. 138-151, 160, Beijing/China.

[23] Zhang Y.J., Xu H.M., Jay H.K., Liu S., Wang C.L., Jiang W. (2019). Finite element analyses and topology optimization of hammer feed grinder frame plate (锤片式饲料粉碎机架板的有限元分析及拓扑优化). *Journal of Huazhong Agricultural University*. Vol. 38, no.05, pp. 159-167, Hubei/China.

[24] Zartha J.W., Pinto P.J., Palaclo J.C., Rios A.F. (2021). Trends in grinding of agroindustrial products - a literature review. *Recent Patents on Food*, *Nutrition & Agriculture*. Vol. 12, no. 1, pp. 19-28, United Arab Emirates.